


Measurement of the Branching Fractions $\mathcal{B}(B^0 \rightarrow p\bar{p}p\bar{p})$ and $\mathcal{B}(B_s^0 \rightarrow p\bar{p}p\bar{p})$

R. Aaij *et al.**
(LHCb Collaboration)

 (Received 22 November 2022; revised 1 March 2023; accepted 23 March 2023; published 29 August 2023)

Searches for the rare hadronic decays $B^0 \rightarrow p\bar{p}p\bar{p}$ and $B_s^0 \rightarrow p\bar{p}p\bar{p}$ are performed using proton-proton collision data recorded by the LHCb experiment and corresponding to an integrated luminosity of 9 fb^{-1} . Significances of 9.3σ and 4.0σ , including statistical and systematic uncertainties, are obtained for the $B^0 \rightarrow p\bar{p}p\bar{p}$ and $B_s^0 \rightarrow p\bar{p}p\bar{p}$ signals, respectively. The branching fractions are measured relative to the topologically similar normalization decays $B^0 \rightarrow J/\psi(\rightarrow p\bar{p})K^{*0}(\rightarrow K^+\pi^-)$ and $B_s^0 \rightarrow J/\psi(\rightarrow p\bar{p})\times \phi(\rightarrow K^+K^-)$. The branching fractions are measured to be $\mathcal{B}(B^0 \rightarrow p\bar{p}p\bar{p}) = (2.2 \pm 0.4 \pm 0.1 \pm 0.1) \times 10^{-8}$ and $\mathcal{B}(B_s^0 \rightarrow p\bar{p}p\bar{p}) = (2.3 \pm 1.0 \pm 0.2 \pm 0.1) \times 10^{-8}$. In these measurements, the first uncertainty is statistical, the second is systematic, and the third one is due to the external branching fraction of the normalization channel.

DOI: [10.1103/PhysRevLett.131.091901](https://doi.org/10.1103/PhysRevLett.131.091901)

The detailed interplay of weak and strong interactions in B meson decays that leads to charmless, hadronic final states with $p\bar{p}$ pairs, remains poorly understood 35 years after their first observations by the ARGUS Collaboration [1]. The patterns of two-body and multibody final states with baryon-antibaryon pairs suggest that dynamical enhancements at low baryon-antibaryon invariant mass are important in the latter. Pronounced enhancements near threshold were first reported in B decays to the $p\bar{p}K^+$, $p\bar{p}\pi^+$, $p\bar{p}K_s^0$, and $p\bar{p}K^{*+}$ final states by the Belle Collaboration [2,3]. Less significant enhancements were also observed by the BABAR Collaboration in several multibody baryonic B decays [4], and by the Belle Collaboration in B decays to charmed baryons [5]. Various approaches [6–10], including QCD sum rules and perturbative QCD models, have been used to predict the small branching fractions of two-body baryonic B decays. Recent phenomenological papers describe the low-mass baryon-antibaryon enhancements in multibody B decays in terms of gluonic and fragmentation mechanisms [11], pole models [12], or through the presence of an intermediate $X(1835)$ baryonium bound state [13].

Final states with *two* baryon-antibaryon pairs are more mysterious still; no predictions exist yet for such B decays, and experimentally none has been observed. However, they have the potential to constrain or to discriminate between the mechanisms outlined above. For example, if the $p\bar{p}$ enhancement is due to a below-threshold state X , the

process $B \rightarrow XX$ would be an excellent laboratory to constrain its quantum numbers.

The BABAR Collaboration reports an upper limit on the $B^0 \rightarrow p\bar{p}p\bar{p}$ branching fraction of 2×10^{-7} at 90% C.L. [14]. No prior search for $B_s^0 \rightarrow p\bar{p}p\bar{p}$ has been reported. The two-body charmless decays $B^0 \rightarrow p\bar{p}$ are expected to proceed mainly through tree-level W -emission amplitudes [7,15], while $B_s^0 \rightarrow p\bar{p}$ decays are expected to proceed via suppressed topologies [15,16] (Cabibbo- and helicity-suppressed W exchange, Cabibbo-suppressed W emission followed by $s\bar{s} \rightarrow p\bar{p}$ rescattering, or penguin annihilation). The LHCb Collaboration recently measured the $B^0 \rightarrow p\bar{p}$ branching fraction, $(1.27 \pm 0.14) \times 10^{-8}$ [17], and set an upper limit on the $B_s^0 \rightarrow p\bar{p}$ decay of 4.4×10^{-9} at 90% C.L. [17]. By analogy, the branching fraction of $B^0 \rightarrow p\bar{p}p\bar{p}$ decays is expected to be larger than the corresponding B_s^0 decay.

We search for $B_{(s)}^0 \rightarrow p\bar{p}p\bar{p}$ using the full Run 1 and Run 2 proton-proton collision data collected by the LHCb experiment over the period 2011–2018 at center-of-mass energies of 7, 8, and 13 TeV with integrated luminosities of approximately 1, 2, and 6 fb^{-1} , respectively. (Charge-conjugate decays are implied throughout this Letter, unless explicitly stated otherwise.) The $B^0 \rightarrow p\bar{p}p\bar{p}$ and $B_s^0 \rightarrow p\bar{p}p\bar{p}$ yields are determined from fits to the integrated datasets with different selection criteria. Anticipating the B_s^0 signal to be much smaller than the B^0 signal, tighter selection criteria for the B_s^0 study are used to further suppress background.

The branching fractions of the signal decays are measured simultaneously across all data-taking periods relative to the topologically similar $B^0 \rightarrow J/\psi(\rightarrow p\bar{p})K^{*0}(\rightarrow K^+\pi^-)$ and $B_s^0 \rightarrow J/\psi(\rightarrow p\bar{p})\phi(\rightarrow K^+K^-)$ normalization channels using

*Full author list given at the end of the article.

$$\begin{aligned} \mathcal{B}(B^0 \rightarrow p\bar{p}p\bar{p}) &= \mathcal{B}_{\text{vis}}(B^0 \rightarrow J/\psi K^{*0}) \\ &\times \frac{N(B^0 \rightarrow p\bar{p}p\bar{p})}{N(B^0 \rightarrow J/\psi K^{*0})} \times \frac{\epsilon(B^0 \rightarrow J/\psi K^{*0})}{\epsilon(B^0 \rightarrow p\bar{p}p\bar{p})}, \end{aligned} \quad (1)$$

$$\begin{aligned} \mathcal{B}(B_s^0 \rightarrow p\bar{p}p\bar{p}) &= \mathcal{B}_{\text{vis}}(B_s^0 \rightarrow J/\psi\phi) \\ &\times \frac{N(B_s^0 \rightarrow p\bar{p}p\bar{p})}{N(B_s^0 \rightarrow J/\psi\phi)} \times \frac{\epsilon(B_s^0 \rightarrow J/\psi\phi)}{\epsilon(B_s^0 \rightarrow p\bar{p}p\bar{p})}, \end{aligned} \quad (2)$$

where N denotes a measured yield and ϵ denotes a combination of geometrical acceptance of the LHCb detector and reconstruction, trigger, and selection efficiencies. The symbol \mathcal{B}_{vis} denotes the branching fraction of the nominal final state multiplied by the branching fractions of its intermediate-state resonances to their decay products. The normalization channels, $B^0 \rightarrow J/\psi K^{*0}$ and $B_s^0 \rightarrow J/\psi\phi$, are chosen because their branching fractions are well measured: $(1.27 \pm 0.05) \times 10^{-3}$ and $(1.04 \pm 0.04) \times 10^{-3}$, respectively [18]. Simultaneously fitting the ratios of signal $B_{(s)}^0 \rightarrow p\bar{p}p\bar{p}$ rates to normalization channel rates mitigates many of the possible systematic uncertainties. The goal of the analysis presented here is to probe $B_{(s)}^0 \rightarrow p\bar{p}p\bar{p}$ branching fractions with sensitivities of $\mathcal{O}(10^{-8})$, similar to that for $B^0 \rightarrow p\bar{p}$ [17,19].

The LHCb detector [20,21] is a single-arm forward spectrometer covering the pseudorapidity range $2 < \eta < 5$, designed for the study of particles containing b or c quarks. The detector includes a high-precision tracking system consisting of a silicon-strip vertex detector surrounding the pp interaction region [22], a large-area silicon-strip detector located upstream of a dipole magnet with a bending power of about 4 Tm, and three stations of silicon-strip detectors and straw drift tubes [23] placed downstream of the magnet. The tracking system provides the measurements of the track momentum and impact parameter (IP) and is used to reconstruct primary vertices (PVs). Different types of charged hadrons are distinguished using particle identification (PID) information from two ring-imaging Cherenkov detectors [24]. The online event selection is performed by a trigger [25], which consists of a hardware stage followed by a software stage, comprising two levels, which applies a full event reconstruction. All candidates must satisfy at least one of two criteria—either a decision to accept the event was completely *independent* of the tracks used to form the candidate (TIS) or a positive decision was dependent *on* the tracks in the signal and no others (TOS).

Simulated samples are used to study the properties of the signal, normalization, and background channels. Proton-proton collisions are generated by PYTHIA [26] with a specific LHCb configuration [27]. Decays of unstable particles are described by EvtGen [28], in which final-state

radiation is generated using PHOTOS [29]. The interactions of the generated particles with the detector material, and their responses, are implemented using the GEANT4 toolkit [30,31], as described in Ref. [32]. A phase-space decay model is used to generate the signal samples.

In the offline selection, B candidates are formed from tracks required to satisfy quality criteria, and to have a momentum in the range $10 < p < 110$ GeV/ c . Individual track trajectories must be inconsistent with originating at a PV using the criterion $\chi_{\text{IP}}^2 > 25$, where χ_{IP}^2 is the difference between the vertex fit χ^2 of a PV reconstructed with and without the track in question. The distance of closest approach between any two tracks of a B candidate is required to be less than 300 μm . The B candidate momentum is required to point back to its PV by requiring $\chi_{\text{IP}}^2 < 25$. The angle between the candidate momentum vector and the line connecting the associated PV and the decay vertex of the candidate must be less than 14 mrad. The B vertex is required to be well separated from the PV and the B candidate must have a decay time greater than 1.0 ps. For the $p\bar{p}hh'$ data samples additional requirements are made on the final state invariant masses around the known masses of the J/ψ , K^{*0} or ϕ mesons: $|m_{p\bar{p}} - 3097| < 60$, $|m_{K^+\pi^-} - 895.5| < 200$, and $|m_{K^+K^-} - 1019.5| < 30$ MeV/ c^2 .

The two most powerful discriminating variables between signal and background are the χ_{IP}^2 of the $B_{(s)}^0$ candidate with respect to the PV and the quantity $\prod_i \mathcal{P}_i(p)$. The latter is defined as the product of the probabilities of the four protons being correctly identified. Since the PID algorithms were tuned differently for Run 1 and Run 2, $\prod_i \mathcal{P}_i(p)$ is optimized separately for the two running periods. Using $p\bar{p}p\bar{p}$ data in the sideband mass ranges $m(p\bar{p}p\bar{p}) \in (4950 - 5240) \cup (5407 - 5650)$ MeV/ c^2 and simulated B^0 and B_s^0 signals, the selections applied to these variables are chosen to maximize S/\sqrt{B} , where S and B are the signal and background yields in the signal region $m(p\bar{p}p\bar{p}) \in [5240, 5407]$ MeV/ c^2 , with the constraint that $S/\sqrt{S+B}$ is greater than 95% of its maximum value.

The yield of $B^0 \rightarrow p\bar{p}p\bar{p}$ decays is expected to be larger than that of the $B_s^0 \rightarrow p\bar{p}p\bar{p}$ mode, due both to a larger expected branching fraction and the suppression of the B_s^0 production rate by a factor of $f_s/f_d \sim 25\%$ [33] compared to that of B^0 production. Thus, different working points are chosen: *tight* and *very tight* selections for the B^0 and B_s^0 searches, respectively.

Expected signal rates in Run 1 are estimated from a previous study based on Run 1 $p\bar{p}p\bar{p}$ data [34], while those expected in Run 2 are extrapolated from the Run 1 measured $B^0 \rightarrow p\bar{p}p\bar{p}$ yield. Prior to unblinding the Run 1 data, a list of tight and very tight $\prod_i \mathcal{P}_i(p)$ working points for the Run 2 data as a function of a large range of possible central values for the B^0 signal in Run 1 were established. In choosing the working points, only $\prod_i \mathcal{P}_i(p)$ values that

are integer multiples of 0.05 in the range (0.10–0.90) were considered to avoid possible biases associated with fine tuning. The $\prod_i \mathcal{P}_i(p)$ requirement for the very tight selection increases the background rejection by a factor of four while reducing the signal efficiency by $\sim 40\%$ with respect to the tight selection. For the χ_{IP}^2 variable, a common requirement $\chi_{\text{IP}}^2 < 1.8$ is used for both channels in all running periods. Signal and normalization efficiencies are estimated from simulation weighted to match the data distributions of the χ_{IP}^2 of the $B_{(s)}^0$ candidate, the track multiplicity in the event and the momentum and pseudorapidity of each daughter particle. The weights are obtained from background-subtracted normalization data samples with loose requirements applied [all selection criteria except those on $B_{(s)}^0 \chi_{\text{IP}}^2$ and $\prod_i \mathcal{P}_i(p)$]. The ratio of efficiencies, after the full selection, between the signal and corresponding normalization channels are similar and vary according to the data taking conditions: ~ 0.6 in Run 1 and ~ 0.7 in Run 2. The fact that these are not equal to unity is primarily due to differences in reconstruction and PID efficiencies between the final state particles of the signal and normalization channels.

The invariant mass ($m(p\bar{p}p\bar{p})$) distributions of the candidates satisfying the tight and very tight selection criteria are shown in Fig. 1. The candidates selected with the tight (very tight) cuts are used to measure $\mathcal{B}(B^0 \rightarrow p\bar{p}p\bar{p})$ [$\mathcal{B}(B_s^0 \rightarrow p\bar{p}p\bar{p})$]. The fits shown here are used only to determine the statistical significances of the signals. The (common) signal shapes are assumed to be described by double-sided Crystal Ball (DSCB) functions [35] with tail parameters fixed to those found in simulation. The mean of the B^0 mass distribution is Gaussian constrained to the value measured for the normalization channel $B^0 \rightarrow J/\psi K^{*0}$ and the mean of the B_s^0 mass distribution is fixed to that of the B^0 plus the known $B_s^0 - B^0$ mass difference [18]. The signal widths are fixed to the values measured for the corresponding normalization channels scaled by the ratio of

signal to normalization widths measured in the simulation. The background shapes are assumed to be exponential with coefficients that are left free to vary in the fit. The B^0 and B_s^0 signal yields obtained from the fit to the samples with tight and very tight selection criteria are 48.2 ± 8.1 and 7.1 ± 2.9 , respectively, including statistical uncertainties only.

For each channel, the absolute branching fraction is measured from a simultaneous unbinned maximum-likelihood fit to the signal and normalization channels in which the corresponding yields are free to vary [see Eq. (1)]. The data are divided into four running periods during which operating conditions varied (years 2011–2012, 2015–2016, 2017, and 2018); these data are fitted simultaneously. The signal shapes described above are also used in this fit. Common means and widths are used to describe the B^0 and B_s^0 mass distributions between the signal and normalization channels. The B^0 and B_s^0 mass and width parameters vary freely in the fit; they are common to the signal and normalization modes but the signal widths are scaled by the ratio of signal to normalization widths in the simulation. Several shape parameters of the normalization channels are common between the three data-taking periods in Run 2. The efficiencies for both signal and normalization channels are determined separately for each running period.

For each normalization channel, $B^0 \rightarrow J/\psi(\rightarrow p\bar{p}) \times K^{*0}(\rightarrow K^+\pi^-)$ and $B_s^0 \rightarrow J/\psi(\rightarrow p\bar{p})\phi(\rightarrow K^+K^-)$, the signal model for the corresponding $p\bar{p}hh'$ sample is modeled as a three-dimensional (3D) probability density function in $m_{p\bar{p}hh'}$, $m_{p\bar{p}}$, and $m_{hh'}$. The $B^0 \rightarrow J/\psi K^{*0}$ ($B_s^0 \rightarrow J/\psi\phi$) contributions to the $m_{p\bar{p}K^+\pi^-}$ ($m_{p\bar{p}K^+K^-}$) and $m_{p\bar{p}}$ spectra are parametrized using DSCB functions to describe the B^0 (B_s^0) and J/ψ shapes. The J/ψ resonance is very narrow, so its shape is completely dominated by resolution effects. The $K^*(892)^0$ shape in the $m_{K^+\pi^-}$ spectrum is modeled using a relativistic Breit-Wigner (RBW) function. As its natural width is so large, resolution

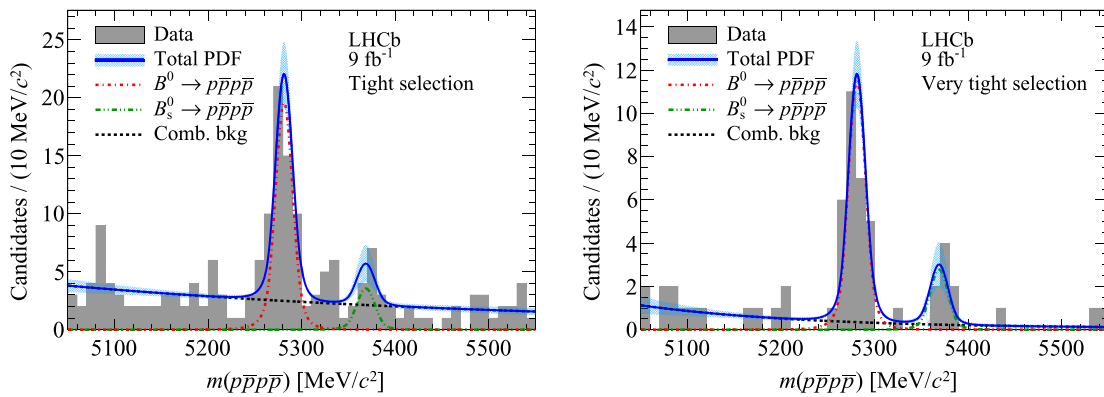


FIG. 1. Combined Run 1 plus Run 2 invariant-mass distributions of $B_{(s)}^0 \rightarrow p\bar{p}p\bar{p}$ candidates satisfying (left) the tight and (right) the very tight selection criteria discussed in the text. The fit results (solid blue lines) for these samples are shown together with the fit model components. The hashed cyan band corresponds to the 1σ model uncertainty based on the fit covariance matrix.

effects are negligible. Since the natural width of the ϕ meson, $\Gamma = (4.23 \pm 0.01) \text{ MeV}/c^2$ [18], is comparable to the expected resolution ($\sim 10 \text{ MeV}/c^2$) obtained from simulation, the $B_s^0 \rightarrow J/\psi\phi$ contribution to the $m_{K^+K^-}$ spectrum is parameterized using a RBW function convolved with a Gaussian function accounting for resolution effects. An S -wave component, denoted $(K\pi)_0$, is modeled in the $m_{K^+\pi^-}$ spectrum distribution using a LASS parametrization that describes nonresonant and $K_0^*(1430)^0$ S -wave contributions [36,37]; this component is modeled in the $p\bar{p}K^+\pi^-$ and $p\bar{p}$ invariant mass distributions with the same shape as the $B^0 \rightarrow J/\psi K^{*0}$ component. The invariant mass distributions of the normalization channels, with the 3D fit projections superimposed from which the $J/\psi K^{*0}$ and $J/\psi\phi$ normalization yields are extracted, are given in the Supplemental Material [38].

Sources of systematic uncertainties from the fit models, the efficiencies as estimated from simulation, particle identification, and the branching fractions of the normalization channels are considered. A summary is presented in Table I. A subset of the systematic uncertainties affects the statistical significances of the $B_{(s)}^0 \rightarrow p\bar{p}p\bar{p}$ yields. The signal shapes are varied in two ways: (i) the DSCB tail parameters are varied and (ii) the DSCB function is replaced with a Johnson SU distribution [39]. The exponential background shapes are replaced with linear shapes. The largest change in the B^0 (B_s^0) yield is $\sim 1\%$ (9%) which we assign as the associated systematic uncertainty. In both cases, the absolute uncertainty in signal yield is ~ 0.5 events, which is negligible compared to the corresponding statistical uncertainties.

Uncertainties on the material budget and particle interaction cross sections lead to uncertainties on the efficiency ratios. These are estimated to be 0.8% and 1.0% for $\mathcal{B}(B^0 \rightarrow p\bar{p}p\bar{p})$ and $\mathcal{B}(B_s^0 \rightarrow p\bar{p}p\bar{p})$, respectively. Differences between PID efficiencies in data and simulation are corrected using a combination of simulated and data calibration samples. The corrections depend on both the sample size of the simulation samples and the kernel

TABLE I. Summary of systematic uncertainties on $\mathcal{B}(B_{(s)}^0 \rightarrow p\bar{p}p\bar{p})$ relative to the statistical uncertainties in [%]. The total systematic uncertainty is calculated as the quadratic sum of the individual systematic uncertainties.

Systematic source	$\mathcal{B}(B^0 \rightarrow p\bar{p}p\bar{p})$	$\mathcal{B}(B_s^0 \rightarrow p\bar{p}p\bar{p})$
Efficiencies (sample size)	5	3
Efficiencies (weights)	16	9
PID	8	3
Tracking	5	2
Fixed PDF parameters	5	2
Signal model	1	4
Background model	8	18
Total systematic	22	21
Normalization \mathcal{B}	24	13

densities used to weight the data calibration samples to match the kinematic distributions of the signals. The overall uncertainties from PID are estimated to be $\sim 1.5\%$ in both cases. Two sources of systematic uncertainties associated with the efficiencies estimated from the simulation are determined. First, the uncertainties on the nominal efficiencies due to the size of the simulated samples are evaluated by applying a Gaussian constraint in the fit. Second, the uncertainties from the weights used to correct discrepancies between simulation and data are conservatively estimated from an alternative fit with unweighted efficiencies, covering possible differences between data and simulation. The corresponding systematic uncertainties on both signal branching fractions are estimated to be $\sim 1\%$ and $\sim 3\%$ for these two sources, respectively. The latter covers uncertainties, of typically $\sim 1\%$, due to imperfect description of the detector in the simulation for relative hardware trigger efficiencies between two topologically similar decay modes [17]. The uncertainties associated with the normalization channel branching fractions are taken from [18].

Finally, potential remaining sources of systematic uncertainties affecting ratios of efficiencies are studied by dividing the data into disjoint samples and comparing the branching fractions measured in each subset. Five sets of disjoint subsamples are defined, with candidates separated according to the two magnet polarities, the four running periods, four bins of candidate B momentum, four bins of candidate B pseudorapidity, and three mutually exclusive hardware trigger categories (TIS only, TOS only, and the overlap between them). For each set of subsamples, i , a p value (p_i) is determined for the hypothesis that the observed variations are consistent with statistical fluctuations using a χ^2 test comparing the nominal branching fractions with those observed in the subsamples. The ensemble p value defined as the product $\prod_i p_i$ is then computed. Ensemble p values of 0.15 and 0.55 are observed for the $\mathcal{B}(B^0 \rightarrow p\bar{p}p\bar{p})$ and $\mathcal{B}(B_s^0 \rightarrow p\bar{p}p\bar{p})$ measurements, respectively, and no additional systematic uncertainties are included.

Using the tight and very tight selections, the $B^0 \rightarrow p\bar{p}p\bar{p}$ and $B_s^0 \rightarrow p\bar{p}p\bar{p}$ branching fractions are measured to be $\mathcal{B}(B^0 \rightarrow p\bar{p}p\bar{p}) = (2.2 \pm 0.4 \pm 0.1 \pm 0.1) \times 10^{-8}$ and $\mathcal{B}(B_s^0 \rightarrow p\bar{p}p\bar{p}) = (2.3 \pm 1.0 \pm 0.2 \pm 0.1) \times 10^{-8}$, where the first uncertainty is statistical, the second is systematic and the third is due to the external branching fraction of the normalization channel. The significances of the $B^0 \rightarrow p\bar{p}p\bar{p}$ and $B_s^0 \rightarrow p\bar{p}p\bar{p}$ signal yields, computed from likelihood scans using Wilks' theorem [40] and accounting for systematic uncertainties associated with signal and background shapes, are 9.3σ and 4.0σ , respectively. The branching fraction ratios are $\mathcal{B}(B^0 \rightarrow p\bar{p}p\bar{p})/\mathcal{B}[B^0 \rightarrow J/\psi(\rightarrow p\bar{p})K^{*0}(\rightarrow K^+\pi^-)] = (1.24 \pm 0.21 \pm 0.04) \times 10^{-2}$ and $\mathcal{B}(B_s^0 \rightarrow p\bar{p}p\bar{p})/\mathcal{B}[B_s^0 \rightarrow J/\psi(\rightarrow p\bar{p})\phi(\rightarrow K^+K^-)] = (2.1 \pm 0.9 \pm 0.2) \times 10^{-2}$,

where the first uncertainty is statistical and the second is systematic.

The sizes of the $p \bar{p} p \bar{p}$ samples are too limited to quantitatively study possible $c\bar{c}$ contributions that might be produced by tree-level, CKM-favored amplitudes, such as $B_s^0 \rightarrow J/\psi(\rightarrow p\bar{p})p\bar{p}$. By excluding $p \bar{p} p \bar{p}$ candidates if any $p \bar{p}$ invariant mass is greater than $2850 \text{ MeV}/c^2$, as shown in the Supplemental Material [38], the data clearly demonstrate the presence of a dominant charmless contribution. With the $c\bar{c}$ veto the efficiencies for pure phase-space decays (ignoring antisymmetrization of amplitudes for fermion pairs) are reduced by 40%–50% according to the simulation. The $B^0 \rightarrow p\bar{p}p\bar{p}$ and $B_s^0 \rightarrow p\bar{p}p\bar{p}$ branching fractions measured with this additional requirement are $(1.6 \pm 0.4) \times 10^{-8}$ and $(2.2 \pm 1.2) \times 10^{-8}$ (statistical uncertainties only), respectively, consistent with those measured over the full phase space. The $B^0 \rightarrow p\bar{p}p\bar{p}$ and $B_s^0 \rightarrow p\bar{p}p\bar{p}$ significances, with the $c\bar{c}$ vetoes applied, are 6.5σ and 3.6σ . A qualitative examination of the $m_{p\bar{p}}$ spectra in the B^0 sample is consistent with $\mathcal{B}(B^0 \rightarrow J/\psi p\bar{p}) \times \mathcal{B}(J/\psi \rightarrow p\bar{p})$ at the expected level of $\mathcal{O}(10^{-9})$ [18]. No evidence for other resonant contributions or a low-mass $p\bar{p}$ enhancement is observed. These observations support the hypothesis that both the $B^0 \rightarrow p\bar{p}p\bar{p}$ and the $B_s^0 \rightarrow p\bar{p}p\bar{p}$ decays proceed primarily through charmless transitions.

In summary, we have searched for the decays $B^0 \rightarrow p\bar{p}p\bar{p}$ and $B_s^0 \rightarrow p\bar{p}p\bar{p}$ using the full LHCb Run 1 and Run 2 datasets and report branching fractions for both. Significances of 9.3σ and 4.0σ , including statistical and systematic uncertainties, are measured for $B^0 \rightarrow p\bar{p}p\bar{p}$ and $B_s^0 \rightarrow p\bar{p}p\bar{p}$ signals, respectively. The measured $\mathcal{B}(B^0 \rightarrow p\bar{p}p\bar{p})$ is about an order of magnitude lower than the upper limit previously reported by the BABAR Collaboration and about twice that of the $B^0 \rightarrow p\bar{p}$ decay while the measured $\mathcal{B}(B_s^0 \rightarrow p\bar{p}p\bar{p})$ is about four times the upper limit for the $B_s^0 \rightarrow p\bar{p}$ decay.

No evidence for resonant substructure associated with either decay is observed. The data suggest that $\mathcal{B}(B_s^0 \rightarrow p\bar{p}p\bar{p})$ is of the same order of magnitude as $\mathcal{B}(B^0 \rightarrow p\bar{p}p\bar{p})$, an unanticipated result. A branching fraction as large as $\mathcal{O}(10^{-8})$ for the B_s^0 decay is difficult to explain as either a Cabibbo- and helicity-suppressed W -exchange amplitude or a Cabibbo-suppressed W -emission amplitude followed by $s\bar{s}$ scattering to a nonstrange or hidden strangeness final state. The datasets anticipated from Run 3, with a factor of 10 greater signal than for Run 2, should be large enough to study the amplitude structures of $B^0 \rightarrow p\bar{p}p\bar{p}$ decays and to investigate low-mass enhancements, as well as to confirm or definitively exclude the large $B_s^0 \rightarrow p\bar{p}p\bar{p}$ branching fraction suggested by the current data.

We express our gratitude to our colleagues in the CERN accelerator departments for the excellent performance of

the LHC. We thank the technical and administrative staff at the LHCb institutes. We acknowledge support from CERN and from the national agencies: CAPES, CNPq, FAPERJ, and FINEP (Brazil); MOST and NSFC (China); CNRS/IN2P3 (France); BMBF, DFG, and MPG (Germany); INFN (Italy); NWO (Netherlands); MNiSW and NCN (Poland); MEN/IFA (Romania); MICINN (Spain); SNSF and SER (Switzerland); NASU (Ukraine); STFC (United Kingdom); DOE NP and NSF (USA). We acknowledge the computing resources that are provided by CERN, IN2P3 (France), KIT and DESY (Germany), INFN (Italy), SURF (Netherlands), PIC (Spain), GridPP (United Kingdom), CSCS (Switzerland), IFIN-HH (Romania), CBPF (Brazil), Polish WLCG (Poland) and NERSC (USA). We are indebted to the communities behind the multiple open-source software packages on which we depend. Individual groups or members have received support from ARC and ARDC (Australia); Minciencias (Colombia); AvH Foundation (Germany); EPLANET, Marie Skłodowska-Curie Actions, and ERC (European Union); A*MIDEX, ANR, IPhU and Labex P2IO, and Région Auvergne-Rhône-Alpes (France); Key Research Program of Frontier Sciences of CAS, CAS PIFI, CAS CCEPP, Fundamental Research Funds for the Central Universities, and Sci. & Tech. Program of Guangzhou (China); GVA, XuntaGal, GENCAT, and Prog. Atracción Talento, CM (Spain); SRC (Sweden); the Leverhulme Trust, the Royal Society and UKRI (United Kingdom).

-
- [1] H. Albrecht *et al.* (ARGUS Collaboration), Observation of the charmless B meson decays, *Phys. Lett. B* **209**, 119 (1988).
 - [2] K. Abe *et al.* (Belle Collaboration), Observation of $B^\pm \rightarrow p\bar{p}K^\pm$, *Phys. Rev. Lett.* **88**, 181803 (2002).
 - [3] M. Z. Wang *et al.* (Belle Collaboration), Observation of $B^+ \rightarrow p\bar{p}\pi^+$, $B^0 \rightarrow p\bar{p}K^0$, and $B^+ \rightarrow p\bar{p}K^{*+}$, *Phys. Rev. Lett.* **92**, 131801 (2004).
 - [4] P. del Amo Sanchez *et al.* (BABAR Collaboration), Observation and study of the baryonic B -meson decays $B \rightarrow D^{(*)}p\bar{p}(\pi)(\pi)$, *Phys. Rev. D* **85**, 092017 (2012).
 - [5] N. Gabyshev *et al.* (Belle Collaboration), Study of Decay Mechanisms in $B^- \rightarrow \Lambda_c^+ \bar{p}\pi^-$ Decays and Observation of Low-Mass Structure in the $\Lambda_c^+ \bar{p}$ System, *Phys. Rev. Lett.* **97**, 242001 (2006).
 - [6] V. L. Chernyak and I. R. Zhitnitsky, B meson exclusive decays into baryons, *Nucl. Phys.* **B345**, 137 (1990).
 - [7] X.-G. He, T. Li, X.-Q. Li, and Y.-M. Wang, Calculation of $\mathcal{B}(\bar{B}^0 \rightarrow \Lambda_c^+ + \bar{p})$ in the PQCD approach, *Phys. Rev. D* **75**, 034011 (2007).
 - [8] W.-S. Hou and A. Soni, Pathways to Rare Baryonic B Decays, *Phys. Rev. Lett.* **86**, 4247 (2001).
 - [9] Y. K. Hsiao, S.-Y. Tsai, C.-C. Lih, and E. Rodrigues, Testing the W -exchange mechanism with two-body baryonic B decays, *J. High Energy Phys.* **04** (2020) 035.

- [10] H.-Y. Cheng and C.-K. Chua, On the smallness of tree-dominated charmless two-body baryonic B decay rates, *Phys. Rev. D* **91**, 036003 (2015).
- [11] J. L. Rosner, Low mass baryon anti-baryon enhancements in B decays, *Phys. Rev. D* **68**, 014004 (2003).
- [12] M. Suzuki, Partial waves of baryon-antibaryon in three-body B meson decay, *J. Phys. G* **34**, 283 (2007).
- [13] A. Datta and P. J. O'Donnell, A new state of baryonium, *Phys. Lett. B* **567**, 273 (2003).
- [14] J. P. Lees *et al.* (BABAR Collaboration), Search for the decay mode $B^0 \rightarrow pp\bar{p}\bar{p}$, *Phys. Rev. D* **98**, 071102 (2018).
- [15] C.-K. Chua, Charmless two-body baryonic $B_{u,d,s}$ decays revisited, *Phys. Rev. D* **89**, 056003 (2014).
- [16] C.-K. Chua, Rates and CP asymmetries of charmless two-body baryonic $B_{u,d,s}$ decays, *Phys. Rev. D* **95**, 096004 (2017).
- [17] R. Aaij *et al.* (LHCb Collaboration), Search for the rare hadronic decay $B_s^0 \rightarrow p\bar{p}$, *Phys. Rev. D* **108**, 012007 (2023).
- [18] R. L. Workman *et al.* (Particle Data Group), Review of particle physics, *Prog. Theor. Exp. Phys.* **2022**, 083C01 (2022).
- [19] R. Aaij *et al.* (LHCb Collaboration), First Observation of the Rare Purely Baryonic Decay $B^0 \rightarrow p\bar{p}$, *Phys. Rev. Lett.* **119**, 232001 (2017).
- [20] A. A. Alves Jr. *et al.* (LHCb Collaboration), The LHCb detector at the LHC, *J. Instrum.* **3**, S08005 (2008).
- [21] R. Aaij *et al.* (LHCb Collaboration), LHCb detector performance, *Int. J. Mod. Phys. A* **30**, 1530022 (2015).
- [22] R. Aaij *et al.*, Performance of the LHCb vertex locator, *J. Instrum.* **9**, P09007 (2014).
- [23] P. d'Argent *et al.*, Improved performance of the LHCb outer tracker in LHC run 2, *J. Instrum.* **12**, P11016 (2017).
- [24] M. Adinolfi *et al.*, Performance of the LHCb RICH detector at the LHC, *Eur. Phys. J. C* **73**, 2431 (2013).
- [25] R. Aaij *et al.*, The LHCb trigger and its performance in 2011, *J. Instrum.* **8**, P04022 (2013).
- [26] T. Sjöstrand, S. Mrenna, and P. Skands, A brief introduction to PYTHIA 8.1, *Comput. Phys. Commun.* **178**, 852 (2008).
- [27] I. Belyaev *et al.*, Handling of the generation of primary events in Gauss, the LHCb simulation framework, *J. Phys. Conf. Ser.* **331**, 032047 (2011).
- [28] D. J. Lange, The EvtGen particle decay simulation package, *Nucl. Instrum. Methods Phys. Res., Sect. A* **462**, 152 (2001).
- [29] N. Davidson, T. Przedzinski, and Z. Was, PHOTOS interface in C++: Technical and physics documentation, *Comput. Phys. Commun.* **199**, 86 (2016).
- [30] S. Agostinelli *et al.* (Geant4 Collaboration), GEANT4: A simulation toolkit, *Nucl. Instrum. Methods Phys. Res., Sect. A* **506**, 250 (2003).
- [31] J. Allison *et al.* (Geant4 Collaboration), GEANT4 developments and applications, *IEEE Trans. Nucl. Sci.* **53**, 270 (2006).
- [32] M. Clemencic, G. Corti, S. Easo, C. R. Jones, S. Miglioranza, M. Pappagallo, and P. Robbe, The LHCb simulation application, Gauss: Design, evolution and experience, *J. Phys. Conf. Ser.* **331**, 032023 (2011).
- [33] R. Aaij *et al.* (LHCb Collaboration), Precise measurement of the f_s/f_d ratio of fragmentation fractions and of B_s^0 decay branching fractions, *Phys. Rev. D* **104**, 032005 (2021).
- [34] P. A. Wampler, Search for the purely baryonic decays $B_{(s)}^0 \rightarrow p\bar{p}p\bar{p}$, Master thesis, EPFL, 2018 (unpublished).
- [35] T. Skwarnicki, A study of the radiative cascade transitions between the Upsilon-prime and Upsilon resonances, Ph.D. thesis, Institute of Nuclear Physics, Krakow, 1986 [Report No. DESY-F31-86-02].
- [36] D. Aston *et al.*, A study of $K^-\pi^+$ scattering in the reaction $K^-p \rightarrow K^-\pi^+n$ at 11 GeV/c, *Nucl. Phys.* **B296**, 493 (1988).
- [37] B. Aubert *et al.* (BABAR Collaboration), Time-dependent and time-integrated angular analysis of $B \rightarrow \phi K_S^0 \pi^0$ and $B \rightarrow \phi K^+ \pi^-$, *Phys. Rev. D* **78**, 092008 (2008).
- [38] See Supplemental Material at <http://link.aps.org/supplemental/10.1103/PhysRevLett.131.091901> for the normalization channel fit projections and the $p\bar{p}$ invariant-mass distributions in the $p\bar{p}p\bar{p}$ sample.
- [39] N. L. Johnson, Systems of frequency curves generated by methods of translation, *Biometrika* **36**, 149 (1949).
- [40] S. S. Wilks, The large-sample distribution of the likelihood ratio for testing composite hypotheses, *Ann. Math. Stat.* **9**, 60 (1938).

R. Aaij³², A. S. W. Abdelmotteleb⁵⁰, C. Abellan Beteta⁴⁴, F. Abudinén⁵⁰, T. Ackernley⁵⁴, B. Adeva⁴⁰, M. Adinolfi⁴⁸, P. Adlarson⁷⁷, H. Afsharnia⁹, C. Agapopoulou¹³, C. A. Aidala⁷⁸, Z. Ajaltouni⁹, S. Akar⁵⁹, K. Akiba³², J. Albrecht¹⁵, F. Alessio⁴², M. Alexander⁵³, A. Alfonso Alberio³⁹, Z. Aliouche⁵⁶, P. Alvarez Cartelle⁴⁹, R. Amalric¹³, S. Amato², J. L. Amey⁴⁸, Y. Amhis^{11,42}, L. An⁴², L. Anderlini²², M. Andersson⁴⁴, A. Andreianov³⁸, M. Andreotti²¹, D. Andreou⁶², D. Ao⁶, F. Archilli¹⁷, A. Artamonov³⁸, M. Artuso⁶², E. Aslanides¹⁰, M. Atzeni⁴⁴, B. Audurier¹², S. Bachmann¹⁷, M. Bachmayer⁴³, J. J. Back⁵⁰, A. Bailly-reyre¹³, P. Baladron Rodriguez⁴⁰, V. Balagura¹², W. Baldini²¹, J. Baptista de Souza Leite¹, M. Barbetti^{22,b}, R. J. Barlow⁵⁶, S. Barsuk¹¹, W. Barter⁵⁵, M. Bartolini⁴⁹, F. Baryshnikov³⁸, J. M. Basels¹⁴, G. Bassi^{29,c}, B. Batsukh⁴, A. Battig¹⁵, A. Bay⁴³, A. Beck⁵⁰, M. Becker¹⁵, F. Bedeschi²⁹, I. B. Bediaga¹, A. Beiter⁶², V. Belavin³⁸, S. Belin⁴⁰, V. Bellee⁴⁴, K. Belous³⁸, I. Belov³⁸, I. Belyaev³⁸, G. Benane¹⁰, G. Bencivenni²³, E. Ben-Haim¹³, A. Berezhnoy³⁸, R. Bernet⁴⁴, S. Bernet Andres⁷⁶, D. Berninghoff¹⁷

H. C. Bernstein,⁶² C. Bertella,⁵⁶ A. Bertolin,²⁸ C. Betancourt,⁴⁴ F. Betti,⁴² Ia. Bezshyiko,⁴⁴ S. Bhasin,⁴⁸ J. Bhom,³⁵ L. Bian,⁶⁸ M. S. Bieker,¹⁵ N. V. Biesuz,²¹ S. Bifani,⁴⁷ P. Billoir,¹³ A. Biolchini,³² M. Birch,⁵⁵ F. C. R. Bishop,⁴⁹ A. Bitadze,⁵⁶ A. Bizzeti,¹⁵ M. P. Blago,⁴⁹ T. Blake,⁵⁰ F. Blanc,⁴³ J. E. Blank,¹⁵ S. Blusk,⁶² D. Bobulska,⁵³ J. A. Boelhauve,¹⁵ O. Boente Garcia,¹² T. Boettcher,⁵⁹ A. Boldyrev,³⁸ C. S. Bolognani,⁷⁴ R. Bolzonella,^{21,d} N. Bondar,^{38,42} F. Borgato,²⁸ S. Borghi,⁵⁶ M. Borsato,¹⁷ J. T. Borsuk,³⁵ S. A. Bouchiba,⁴³ T. J. V. Bowcock,⁵⁴ A. Boyer,⁴² C. Bozzi,²¹ M. J. Bradley,⁵⁵ S. Braun,⁶⁰ A. Brea Rodriguez,⁴⁰ J. Breckenridge,⁵⁹ J. Brodzicka,³⁵ A. Brossa Gonzalo,⁴⁰ J. Brown,⁵⁴ D. Brundu,²⁷ A. Buonauro,⁴⁴ L. Buonincontri,²⁸ A. T. Burke,⁵⁶ C. Burr,⁴² A. Bursche,⁶⁶ A. Butkevich,³⁸ J. S. Butter,³² J. Buytaert,⁴² W. Byczynski,⁴² S. Cadeddu,²⁷ H. Cai,⁶⁸ R. Calabrese,^{21,d} L. Calefice,¹⁵ S. Cali,²³ R. Calladine,⁴⁷ M. Calvi,^{26,e} M. Calvo Gomez,⁷⁶ P. Campana,²³ D. H. Campora Perez,⁷⁴ A. F. Campoverde Quezada,⁶ S. Capelli,^{26,e} L. Capriotti,²⁰ A. Carbone,^{20,f} G. Carboni,³¹ R. Cardinale,^{24,g} A. Cardini,²⁷ P. Carniti,^{26,e} L. Carus,¹⁴ A. Casais Vidal,⁴⁰ R. Caspary,¹⁷ G. Casse,⁵⁴ M. Cattaneo,⁴² G. Cavallero,⁴² V. Cavallini,^{21,d} S. Celani,⁴³ J. Cerasoli,¹⁰ D. Cervenkov,⁵⁷ A. J. Chadwick,⁵⁴ M. G. Chapman,⁴⁸ M. Charles,¹³ Ph. Charpentier,⁴² C. A. Chavez Barajas,⁵⁴ M. Chefdeville,⁸ C. Chen,³ S. Chen,⁴ A. Chernov,³⁵ S. Chernyshenko,⁴⁶ V. Chobanova,⁴⁰ S. Cholak,⁴³ M. Chrzaszcz,³⁵ A. Chubykin,³⁸ V. Chulikov,³⁸ P. Ciambone,²³ M. F. Cicala,⁵⁰ X. Cid Vidal,⁴⁰ G. Ciezarek,⁴² G. Ciullo,^{21,d} P. E. L. Clarke,⁵² M. Clemencic,⁴² H. V. Cliff,⁴⁹ J. Closier,⁴² J. L. Cobbletick,⁵⁶ V. Coco,⁴² J. A. B. Coelho,¹¹ J. Cogan,¹⁰ E. Cogneras,⁹ L. Cojocariu,³⁷ B. Collins,⁵⁹ P. Collins,⁴² T. Colombo,⁴² L. Congedo,¹⁹ A. Contu,²⁷ N. Cooke,⁴⁷ I. Corredoira,⁴⁰ G. Corti,⁴² B. Couturier,⁴² D. C. Craik,⁴⁴ M. Cruz Torres,^{1,h} R. Currie,⁵² C. L. Da Silva,⁶¹ S. Dadabaev,³⁸ L. Dai,⁶⁵ X. Dai,⁵ E. Dall'Occo,¹⁵ J. Dalseno,⁴⁰ C. D'Ambrosio,⁴² J. Daniel,⁹ A. Danilina,³⁸ P. d'Argent,¹⁵ J. E. Davies,⁵⁶ A. Davis,⁵⁶ O. De Aguiar Francisco,⁵⁶ J. de Boer,⁴² K. De Bruyn,⁷³ S. De Capua,⁵⁶ M. De Cian,⁴³ U. De Freitas Carneiro Da Graca,¹ E. De Lucia,²³ J. M. De Miranda,¹ L. De Paula,² M. De Serio,^{19,i} D. De Simone,⁴⁴ P. De Simone,²³ F. De Vellis,¹⁵ J. A. de Vries,⁷⁴ C. T. Dean,⁶¹ F. Debernardis,^{19,i} D. Decamp,⁸ V. Dedu,¹⁰ L. Del Buono,¹³ B. Delaney,⁵⁸ H.-P. Dembinski,¹⁵ V. Denysenko,⁴⁴ O. Deschamps,⁹ F. Dettori,^{27,j} B. Dey,⁷¹ P. Di Nezza,²³ I. Diachkov,³⁸ S. Didenko,³⁸ L. Dieste Maronas,⁴⁰ S. Ding,⁶² V. Dobishuk,⁴⁶ A. Dolmatov,³⁸ C. Dong,³ A. M. Donohoe,¹⁸ F. Dordei,²⁷ A. C. dos Reis,¹ L. Douglas,⁵³ A. G. Downes,⁸ P. Duda,⁷⁵ M. W. Dudek,³⁵ L. Dufour,⁴² V. Duk,⁷² P. Durante,⁴² M. M. Duras,⁷⁵ J. M. Durham,⁶¹ D. Dutta,⁵⁶ A. Dziurda,³⁵ A. Dzyuba,³⁸ S. Easo,⁵¹ U. Egede,⁶³ V. Egorychev,³⁸ S. Eidelman,^{38,a} C. Eirea Orro,⁴⁰ S. Eisenhardt,⁵² E. Ejopu,⁵⁶ S. Ek-In,⁴³ L. Eklund,⁷⁷ S. Ely,⁶² A. Ene,³⁷ E. Epple,⁵⁹ S. Escher,¹⁴ J. Eschle,⁴⁴ S. Esen,⁴⁴ T. Evans,⁵⁶ F. Fabiano,^{27,j} L. N. Falcao,¹ Y. Fan,⁶ B. Fang,^{11,68} L. Fantini,^{72,k} M. Faria,⁴³ S. Farry,⁵⁴ D. Fazzini,^{26,e} L. Felkowski,⁷⁵ M. Feo,⁴² M. Fernandez Gomez,⁴⁰ A. D. Fernez,⁶⁰ F. Ferrari,²⁰ L. Ferreira Lopes,⁴³ F. Ferreira Rodrigues,² S. Ferreres Sole,³² M. Ferrillo,⁴⁴ M. Ferro-Luzzi,⁴² S. Filippov,³⁸ R. A. Fini,¹⁹ M. Fiorini,^{21,d} M. Firlej,³⁴ K. M. Fischer,⁵⁷ D. S. Fitzgerald,⁷⁸ C. Fitzpatrick,⁵⁶ T. Fiutowski,³⁴ F. Fleuret,¹² M. Fontana,¹³ F. Fontanelli,^{24,g} R. Forty,⁴² D. Foulds-Holt,⁴⁹ V. Franco Lima,⁵⁴ M. Franco Sevilla,⁶⁰ M. Frank,⁴² E. Franzoso,^{21,d} G. Frau,¹⁷ C. Frei,⁴² D. A. Friday,⁵³ J. Fu,⁶ Q. Fuehring,¹⁵ T. Fulghesu,¹³ E. Gabriel,³² G. Galati,^{19,i} M. D. Galati,³² A. Gallas Torreira,⁴⁰ D. Galli,^{20,f} S. Gambetta,^{52,42} Y. Gan,³ M. Gandelman,² P. Gandini,²⁵ Y. Gao,⁷ Y. Gao,⁵ M. Garau,^{27,j} L. M. Garcia Martin,⁵⁰ P. Garcia Moreno,³⁹ J. García Pardiñas,^{26,e} B. Garcia Plana,⁴⁰ F. A. Garcia Rosales,¹² L. Garrido,³⁹ C. Gaspar,⁴² R. E. Geertsema,³² D. Gerick,¹⁷ L. L. Gerken,¹⁵ E. Gersabeck,⁵⁶ M. Gersabeck,⁵⁶ T. Gershon,⁵⁰ L. Giambastiani,²⁸ V. Gibson,⁴⁹ H. K. Giemza,³⁶ A. L. Gilman,⁵⁷ M. Giovannetti,^{23,1} A. Gioventù,⁴⁰ P. Gironella Gironell,³⁹ C. Giugliano,^{21,d} M. A. Giza,³⁵ K. Gizdov,⁵² E. L. Gkougkousis,⁴² V. V. Gligorov,^{13,42} C. Göbel,⁶⁴ E. Golobardes,⁷⁶ D. Golubkov,³⁸ A. Golutvin,^{55,38} A. Gomes,^{1,1,2,a,m,n,m} S. Gomez Fernandez,³⁹ F. Goncalves Abrantes,⁵⁷ M. Goncerz,³⁵ G. Gong,³ I. V. Gorelov,³⁸ C. Gotti,²⁶ J. P. Grabowski,⁷⁰ T. Grammatico,¹³ L. A. Granado Cardoso,⁴² E. Graugés,³⁹ E. Graverini,⁴³ G. Graziani,¹⁰ A. T. Grecu,³⁷ L. M. Greeven,³² N. A. Grieser,⁴ L. Grillo,⁵³ S. Gromov,³⁸ B. R. Gruberg Cazon,⁵⁷ C. Gu,³ M. Guarise,^{21,d} M. Guittiere,¹¹ P. A. Günther,¹⁷ E. Gushchin,³⁸ A. Guth,¹⁴ Y. Guz,³⁸ T. Gys,⁴² T. Hadavizadeh,⁶³ C. Hadjivasiliou,⁶⁰ G. Haefeli,⁴³ C. Haen,⁴² J. Haimberger,⁴² S. C. Haines,⁴⁹ T. Halewood-leagas,⁵⁴ M. M. Halvorsen,⁴² P. M. Hamilton,⁶⁰ J. Hammerich,⁵⁴ Q. Han,⁷ X. Han,¹⁷ E. B. Hansen,⁵⁶ S. Hansmann-Menzemer,¹⁷ L. Hao,⁶ N. Harnew,⁵⁷ T. Harrison,⁵⁴ C. Hasse,⁴² M. Hatch,⁴² J. He,^{6,o} K. Heijhoff,³² C. Henderson,⁵⁹ R. D. L. Henderson,^{63,50} A. M. Hennequin,⁵⁸ K. Hennessy,⁵⁴ L. Henry,⁴²

J. Herd⁵⁵, J. Heuel¹⁴, A. Hicheur², D. Hill⁴³, M. Hilton⁵⁶, S. E. Hollitt¹⁵, J. Horswill⁵⁶, R. Hou⁷, Y. Hou⁸, J. Hu¹⁷, J. Hu⁶⁶, W. Hu⁵, X. Hu³, W. Huang⁶, X. Huang⁶⁸, W. Hulsbergen³², R. J. Hunter⁵⁰, M. Hushchyn³⁸, D. Hutchcroft⁵⁴, P. Ibis¹⁵, M. Idzik³⁴, D. Ilin³⁸, P. Ilten⁵⁹, A. Inglessi³⁸, A. Iniukhin³⁸, A. Ishteev³⁸, K. Ivshin³⁸, R. Jacobsson⁴², H. Jage¹⁴, S. J. Jaimes Elles⁴¹, S. Jakobsen⁴², E. Jans³², B. K. Jashal⁴¹, A. Jawahery⁶⁰, V. Jevtic¹⁵, E. Jiang⁶⁰, X. Jiang^{4,6}, Y. Jiang⁶, M. John⁵⁷, D. Johnson⁵⁸, C. R. Jones⁴⁹, T. P. Jones⁵⁰, B. Jost⁴², N. Jurik⁴², I. Juszcak³⁵, S. Kandybei⁴⁵, Y. Kang³, M. Karacson⁴², D. Karpenkov³⁸, M. Karpov³⁸, J. W. Kautz⁵⁹, F. Keizer⁴², D. M. Keller⁶², M. Kenzie⁵⁰, T. Ketel³², B. Khanji¹⁵, A. Kharisova³⁸, S. Kholodenko³⁸, G. Khreich¹¹, T. Kim¹⁴, V. S. Kirsebom⁴³, O. Kitouni⁵⁸, S. Klaver³³, N. Kleijne^{29,c}, K. Klimaszewski³⁶, M. R. Kmiec³⁶, S. Koliiev⁴⁶, A. Kondybayeva³⁸, A. Konoplyannikov³⁸, P. Kopciwicz³⁴, R. Kopecna¹⁷, P. Koppenburg³², M. Korolev³⁸, I. Kostiuk^{32,46}, O. Kot⁴⁶, S. Kotriakhova³⁸, A. Kozachuk³⁸, P. Kravchenko³⁸, L. Kravchuk³⁸, R. D. Krawczyk⁴², M. Kreps⁵⁰, S. Kretzschmar¹⁴, P. Krokovny³⁸, W. Krupa³⁴, W. Krzemien³⁶, J. Kubat¹⁷, S. Kubis⁷⁵, W. Kucewicz^{35,34}, M. Kucharczyk³⁵, V. Kudryavtsev³⁸, A. Kupsc⁷⁷, D. Lacarrere⁴², G. Lafferty⁵⁶, A. Lai²⁷, A. Lampis^{27,j}, D. Lancierini⁴⁴, C. Landesa Gomez⁴⁰, J. J. Lane⁵⁶, R. Lane⁴⁸, G. Lanfranchi²³, C. Langenbruch¹⁴, J. Langer¹⁵, O. Lantwin³⁸, T. Latham⁵⁰, F. Lazzari^{29,p}, M. Lazzaroni^{25,q}, R. Le Gac¹⁰, S. H. Lee⁷⁸, R. Lefèvre⁹, A. Leflat³⁸, S. Legotin³⁸, P. Lenisa^{21,d}, O. Leroy¹⁰, T. Lesiak³⁵, B. Leverington¹⁷, A. Li³, H. Li⁶⁶, K. Li⁷, P. Li¹⁷, P.-R. Li⁶⁷, S. Li⁷, T. Li⁴, T. Li⁶⁶, Y. Li⁴, Z. Li⁶², X. Liang⁶², C. Lin⁶, T. Lin⁵¹, R. Lindner⁴², V. Lisovskyi¹⁵, R. Litvinov^{27,j}, G. Liu⁶⁶, H. Liu⁶, Q. Liu⁶, S. Liu^{4,6}, A. Lobo Salvia³⁹, A. Loi²⁷, R. Lollini⁷², J. Lomba Castro⁴⁰, I. Longstaff⁵³, J. H. Lopes², A. Lopez Huertas³⁹, S. López Soliño⁴⁰, G. H. Lovell⁴⁹, Y. Lu^{4,r}, C. Lucarelli^{22,b}, D. Lucchesi^{28,s}, S. Luchuk³⁸, M. Lucio Martinez⁷⁴, V. Lukashenko^{32,46}, Y. Luo³, A. Lupato⁵⁶, E. Luppi^{21,d}, A. Lusiani^{29,c}, K. Lynch¹⁸, X.-R. Lyu⁶, L. Ma⁴, R. Ma⁶, S. Maccolini²⁰, F. Machefert¹¹, F. Maciuc³⁷, I. Mackay⁵⁷, V. Macko⁴³, P. Mackowiak¹⁵, L. R. Madhan Mohan⁴⁸, A. Maevskiy³⁸, D. Maisuzenko³⁸, M. W. Majewski³⁴, J. J. Malczewski³⁵, S. Malde⁵⁷, B. Malecki^{35,42}, A. Malinin³⁸, T. Maltsev³⁸, G. Manca^{27,j}, G. Mancinelli¹⁰, C. Mancuso^{11,25,q}, D. Manuzzi²⁰, C. A. Manzari⁴⁴, D. Marangotto^{25,q}, J. F. Marchand⁸, U. Marconi²⁰, S. Mariani^{22,b}, C. Marin Benito³⁹, J. Marks¹⁷, A. M. Marshall⁴⁸, P. J. Marshall⁵⁴, G. Martelli^{72,k}, G. Martellotti³⁰, L. Martinazzoli^{42,e}, M. Martinelli^{26,e}, D. Martinez Santos⁴⁰, F. Martinez Vidal⁴¹, A. Massafferri¹, M. Materok¹⁴, R. Matev⁴², A. Mathad⁴⁴, V. Matiunin³⁸, C. Matteuzzi²⁶, K. R. Mattioli¹², A. Mauri³², E. Maurice¹², J. Mauricio³⁹, M. Mazurek⁴², M. McCann⁵⁵, L. McConnell¹⁸, T. H. McGrath⁵⁶, N. T. McHugh⁵³, A. McNab⁵⁶, R. McNulty¹⁸, J. V. Mead⁵⁴, B. Meadows⁵⁹, G. Meier¹⁵, D. Melnychuk³⁶, S. Meloni^{26,e}, M. Merk^{32,74}, A. Merli^{25,q}, L. Meyer Garcia², D. Miao^{4,6}, M. Mikhasenko^{70,t}, D. A. Milanes⁶⁹, E. Millard⁵⁰, M. Milovanovic⁴², M.-N. Minard^{8,a}, A. Minotti^{26,e}, T. Miralles⁹, S. E. Mitchell⁵², B. Mitreska⁵⁶, D. S. Mitzel¹⁵, A. Mödden¹⁵, R. A. Mohammed⁵⁷, R. D. Moise¹⁴, S. Mokhnenko³⁸, T. Mombächer⁴⁰, M. Monk^{50,63}, I. A. Monroy⁶⁹, S. Monteil⁹, M. Morandin²⁸, G. Morello²³, M. J. Morello^{29,c}, J. Moron³⁴, A. B. Morris⁷⁰, A. G. Morris⁵⁰, R. Mountain⁶², H. Mu³, E. Muhammad⁵⁰, F. Muheim⁵², M. Mulder⁷³, K. Müller⁴⁴, C. H. Murphy⁵⁷, D. Murray⁵⁶, R. Murta⁵⁵, P. Muzzetto^{27,j}, P. Naik⁴⁸, T. Nakada⁴³, R. Nandakumar⁵¹, T. Nanut⁴², I. Nasteva², M. Needham⁵², N. Neri^{25,q}, S. Neubert⁷⁰, N. Neufeld⁴², P. Neustroev³⁸, R. Newcombe⁵⁵, J. Nicolini^{15,11}, E. M. Niel⁴³, S. Nieswand¹⁴, N. Nikitin³⁸, N. S. Nolte⁵⁸, C. Normand^{8,27,j}, J. Novoa Fernandez⁴⁰, C. Nunez⁷⁸, A. Oblakowska-Mucha³⁴, V. Obraztsov³⁸, T. Oeser¹⁴, D. P. O'Hanlon⁴⁸, S. Okamura^{21,d}, R. Oldeman^{27,j}, F. Oliva⁵², C. J. G. Onderwater⁷³, R. H. O'Neil⁵², J. M. Otalora Goicochea², T. Ovsianikova³⁸, P. Owen⁴⁴, A. Oyanguren⁴¹, O. Ozelik⁵², K. O. Padeken⁷⁰, B. Pagare⁵⁰, P. R. Pais⁴², T. Pajero⁵⁷, A. Palano¹⁹, M. Palutan²³, Y. Pan⁵⁶, G. Panshin³⁸, L. Paolucci⁵⁰, A. Papanestis⁵¹, M. Pappagallo^{19,i}, L. L. Pappalardo^{21,d}, C. Pappenheimer⁵⁹, W. Parker⁶⁰, C. Parkes^{56,42}, B. Passalacqua^{21,d}, G. Passaleva²², A. Pastore¹⁹, M. Patel⁵⁵, C. Patrignani^{20,f}, C. J. Pawley⁷⁴, A. Pearce⁴², A. Pellegrino³², M. Pepe Altarelli⁴², S. Perazzini²⁰, D. Pereima³⁸, A. Pereiro Castro⁴⁰, P. Perret⁹, M. Petric⁵³, K. Petridis⁴⁸, A. Petrolini^{24,g}, A. Petrov³⁸, S. Petrucci⁵², M. Petruzzo²⁵, H. Pham⁶², A. Philippov³⁸, R. Piandani⁶, L. Pica^{29,c}, M. Piccini⁷², B. Pietrzyk⁸, G. Pietrzyk¹¹, M. Pili⁵⁷, D. Pinci³⁰, F. Pisani⁴², M. Pizzichemi^{26,42,e}, V. Placinta³⁷, J. Plews⁴⁷, M. Plo Casasus⁴⁰, F. Polci^{13,42}, M. Poli Lener²³, M. Poliakova⁶², A. Poluektov¹⁰, N. Polukhina³⁸, I. Polyakov⁴², E. Polycarpo², S. Ponce⁴², D. Popov^{6,42}, S. Popov³⁸, S. Poslavskii³⁸, K. Prasanth³⁵, L. Promberger¹⁷, C. Prouve⁴⁰, V. Pugatch⁴⁶, V. Puill¹¹, G. Punzi^{29,u}, H. R. Qi³, W. Qian⁶, N. Qin³, S. Qu³, R. Quagliani⁴³, N. V. Raab¹⁸

R. I. Rabadan Trejo⁶, B. Rachwal³⁴, J. H. Rademacker⁴⁸, R. Rajagopalan⁶², M. Rama²⁹, M. Ramos Pernas¹⁰, M. S. Rangel², F. Ratnikov³⁸, G. Raven^{33,42}, M. Rebollo De Miguel⁴¹, F. Redi⁴², J. Reich⁴⁸, F. Reiss⁵⁶, C. Remon Alepuz⁴¹, Z. Ren³, P. K. Resmi¹⁰, R. Ribatti^{29,c}, A. M. Ricci²⁷, S. Ricciardi⁵¹, K. Richardson⁵⁸, M. Richardson-Slipper⁵², K. Rinnert⁵⁴, P. Robbe¹¹, G. Robertson⁵², A. B. Rodrigues⁴³, E. Rodrigues⁵⁴, E. Rodriguez Fernandez⁴⁰, J. A. Rodriguez Lopez⁶⁹, E. Rodriguez Rodriguez⁴⁰, D. L. Rolf⁴², A. Rollings⁵⁷, P. Roloff⁴², V. Romanovskiy³⁸, M. Romero Lamas⁴⁰, A. Romero Vidal⁴⁰, J. D. Roth^{78,a}, M. Rotondo²³, M. S. Rudolph⁶², T. Ruf⁴², R. A. Ruiz Fernandez⁴⁰, J. Ruiz Vidal⁴¹, A. Ryzhikov³⁸, J. Ryzka³⁴, J. J. Saborido Silva⁴⁰, N. Sagidova³⁸, N. Sahoo⁴⁷, B. Saitta^{27,j}, M. Salomoni⁴², C. Sanchez Gras³², I. Sanderswood⁴¹, R. Santacesaria³⁰, C. Santamarina Rios⁴⁰, M. Santimaria²³, E. Santovetti^{31,i}, D. Saranin³⁸, G. Sarpis¹⁴, M. Sarpis⁷⁰, A. Sarti³⁰, C. Satriano^{30,v}, A. Satta³¹, M. Saur¹⁵, D. Savrina³⁸, H. Sazak⁹, L. G. Scantlebury Smead⁵⁷, A. Scarabotto¹³, S. Schael¹⁴, S. Scherl⁵⁴, M. Schiller⁵³, H. Schindler⁴², M. Schmelling¹⁶, B. Schmidt⁴², S. Schmitt¹⁴, O. Schneider⁴³, A. Schopper⁴², M. Schubiger³², S. Schulte⁴³, M. H. Schune¹¹, R. Schwemmer⁴², B. Sciascia^{23,42}, A. Sciucati⁴², S. Sellam⁴⁰, A. Semennikov³⁸, M. Senghi Soares³³, A. Sergi^{24,g}, N. Serra⁴⁴, L. Sestini²⁸, A. Seuthe¹⁵, Y. Shang⁵, D. M. Shangase⁷⁸, M. Shapkin³⁸, I. Shchemerov³⁸, L. Shchutska⁴³, T. Shears⁵⁴, L. Shekhtman³⁸, Z. Shen⁵, S. Sheng^{4,6}, V. Shevchenko³⁸, B. Shi⁶, E. B. Shields^{26,e}, Y. Shimizu¹¹, E. Shmanin³⁸, R. Shorkin³⁸, J. D. Shupperd⁶², B. G. Siddi^{21,d}, R. Silva Coutinho⁶², G. Simi²⁸, S. Simone^{19,i}, M. Singla⁶³, N. Skidmore⁵⁶, R. Skuza¹⁷, T. Skwarnicki⁶², M. W. Slater⁴⁷, J. C. Smallwood⁵⁷, J. G. Smeaton⁴⁹, E. Smith⁴⁴, K. Smith⁶¹, M. Smith⁵⁵, A. Snoch³², L. Soares Lavra⁹, M. D. Sokoloff⁵⁹, F. J. P. Soler⁵³, A. Solomin^{38,48}, A. Solovev³⁸, I. Solovyev³⁸, R. Song⁶³, F. L. Souza De Almeida², B. Souza De Paula², B. Spaan^{15,a}, E. Spadaro Norella^{25,q}, E. Spedicato²⁰, E. Spiridenkov³⁸, P. Spradlin⁵³, V. Sriskaran⁴², F. Stagni⁴², M. Stahl⁴², S. Stahl⁴², S. Stanislaus⁵⁷, E. N. Stein⁴², O. Steinkamp⁴⁴, O. Stenyakin³⁸, H. Stevens¹⁵, S. Stone^{62,a}, D. Strelakina³⁸, Y. Su⁶, F. Suljik⁵⁷, J. Sun²⁷, L. Sun⁶⁸, Y. Sun⁶⁰, P. Svihra⁵⁶, P. N. Swallow⁴⁷, K. Swientek³⁴, A. Szabelski³⁶, T. Szumlak³⁴, M. Szymanski⁴², Y. Tan³, S. Taneja⁵⁶, M. D. Tat⁵⁷, A. Terentev³⁸, F. Teubert⁴², E. Thomas⁴², D. J. D. Thompson⁴⁷, K. A. Thomson⁵⁴, H. Tilquin⁵⁵, V. Tisserand⁹, S. T'Jampens⁸, M. Tobin⁴, L. Tomassetti^{21,d}, G. Tonani^{25,q}, X. Tong⁵, D. Torres Machado¹, D. Y. Tou³, S. M. Trilov⁴⁸, C. Trippl⁴³, G. Tuci⁶, A. Tully⁴³, N. Tuning³², A. Ukleja³⁶, D. J. Unverzagt¹⁷, A. Usachov³², A. Ustyuzhanin³⁸, U. Uwer¹⁷, A. Vagner³⁸, V. Vagnoni²⁰, A. Valassi⁴², G. Valenti²⁰, N. Valls Canudas⁷⁶, M. van Beuzekom³², M. Van Dijk⁴³, H. Van Hecke⁶¹, E. van Herwijnen⁵⁵, C. B. Van Hulse^{40,w}, M. van Veghel⁷³, R. Vazquez Gomez³⁹, P. Vazquez Regueiro⁴⁰, C. Vázquez Sierra⁴², S. Vecchi²¹, J. J. Velthuis⁴⁸, M. Veltri^{22,x}, A. Venkateswaran⁴³, M. Veronesi³², M. Vesterinen⁵⁰, D. Vieira⁵⁹, M. Vieites Diaz⁴³, X. Vilasis-Cardona⁷⁶, E. Vilella Figueras⁵⁴, A. Villa²⁰, P. Vincent¹³, F. C. Volle¹¹, D. vom Bruch¹⁰, A. Vorobyev³⁸, V. Vorobyev³⁸, N. Voropaev³⁸, K. Vos⁷⁴, C. Vrahas⁵², R. Waldi¹⁷, J. Walsh²⁹, G. Wan⁵, C. Wang¹⁷, G. Wang⁷, J. Wang⁵, J. Wang⁴, J. Wang³, J. Wang⁶⁸, M. Wang⁵, R. Wang⁴⁸, X. Wang⁶⁶, Y. Wang⁷, Z. Wang⁴⁴, Z. Wang³, Z. Wang⁶, J. A. Ward^{50,63}, N. K. Watson⁴⁷, D. Websdale⁵⁵, Y. Wei⁵, C. Weisser⁵⁸, B. D. C. Westhenry⁴⁸, D. J. White⁵⁶, M. Whitehead⁵³, A. R. Wiederhold⁵⁰, D. Wiedner¹⁵, G. Wilkinson⁵⁷, M. K. Wilkinson⁵⁹, I. Williams⁴⁹, M. Williams⁵⁸, M. R. J. Williams⁵², R. Williams⁴⁹, F. F. Wilson⁵¹, W. Wislicki³⁶, M. Witek³⁵, L. Witola¹⁷, C. P. Wong⁶¹, G. Wormser¹¹, S. A. Wotton⁴⁹, H. Wu⁶², J. Wu⁷, K. Wyllie⁴², Z. Xiang⁶, D. Xiao⁷, Y. Xie⁷, A. Xu⁵, J. Xu⁶, L. Xu³, L. Xu³, M. Xu⁵⁰, Q. Xu⁶, Z. Xu⁹, Z. Xu⁶, D. Yang³, S. Yang⁶, X. Yang⁵, Y. Yang⁶, Z. Yang⁵, Z. Yang⁶⁰, L. E. Yeomans⁵⁴, V. Yeroshenko¹¹, H. Yeung⁵⁶, H. Yin⁷, J. Yu⁶⁵, X. Yuan⁶², E. Zaffaroni⁴³, M. Zavertyaev¹⁶, M. Zdybal³⁵, O. Zenaiev⁴², M. Zeng³, C. Zhang⁵, D. Zhang⁷, L. Zhang³, S. Zhang⁶⁵, S. Zhang⁵, Y. Zhang⁵, Y. Zhang⁵⁷, H. Zhao⁶⁵, A. Zharkova³⁸, A. Zhelezov¹⁷, Y. Zheng⁶, T. Zhou⁵, X. Zhou⁶, Y. Zhou⁶, V. Zhovkovska¹¹, X. Zhu³, X. Zhu⁷, Z. Zhu⁶, V. Zhukov^{14,38}, Q. Zou^{4,6}, S. Zucchelli^{20,f}, D. Zuliani²⁸ and G. Zunica⁵⁶

(LHCb Collaboration)

- ¹*Centro Brasileiro de Pesquisas Físicas (CBPF), Rio de Janeiro, Brazil*
²*Universidade Federal do Rio de Janeiro (UFRJ), Rio de Janeiro, Brazil*
³*Center for High Energy Physics, Tsinghua University, Beijing, China*
⁴*Institute Of High Energy Physics (IHEP), Beijing, China*
⁵*School of Physics State Key Laboratory of Nuclear Physics and Technology, Peking University, Beijing, China*
⁶*University of Chinese Academy of Sciences, Beijing, China*
⁷*Institute of Particle Physics, Central China Normal University, Wuhan, Hubei, China*
⁸*Université Savoie Mont Blanc, CNRS, IN2P3-LAPP, Annecy, France*
⁹*Université Clermont Auvergne, CNRS/IN2P3, LPC, Clermont-Ferrand, France*
¹⁰*Aix Marseille Univ, CNRS/IN2P3, CPPM, Marseille, France*
¹¹*Université Paris-Saclay, CNRS/IN2P3, IJCLab, Orsay, France*
¹²*Laboratoire Leprince-Ringuet, CNRS/IN2P3, Ecole Polytechnique, Institut Polytechnique de Paris, Palaiseau, France*
¹³*LPNHE, Sorbonne Université, Paris Diderot Sorbonne Paris Cité, CNRS/IN2P3, Paris, France*
¹⁴*I. Physikalisches Institut, RWTH Aachen University, Aachen, Germany*
¹⁵*Fakultät Physik, Technische Universität Dortmund, Dortmund, Germany*
¹⁶*Max-Planck-Institut für Kernphysik (MPIK), Heidelberg, Germany*
¹⁷*Physikalisches Institut, Ruprecht-Karls-Universität Heidelberg, Heidelberg, Germany*
¹⁸*School of Physics, University College Dublin, Dublin, Ireland*
¹⁹*INFN Sezione di Bari, Bari, Italy*
²⁰*INFN Sezione di Bologna, Bologna, Italy*
²¹*INFN Sezione di Ferrara, Ferrara, Italy*
²²*INFN Sezione di Firenze, Firenze, Italy*
²³*INFN Laboratori Nazionali di Frascati, Frascati, Italy*
²⁴*INFN Sezione di Genova, Genova, Italy*
²⁵*INFN Sezione di Milano, Milano, Italy*
²⁶*INFN Sezione di Milano-Bicocca, Milano, Italy*
²⁷*INFN Sezione di Cagliari, Monserrato, Italy*
²⁸*Università degli Studi di Padova, Università e INFN, Padova, Padova, Italy*
²⁹*INFN Sezione di Pisa, Pisa, Italy*
³⁰*INFN Sezione di Roma La Sapienza, Roma, Italy*
³¹*INFN Sezione di Roma Tor Vergata, Roma, Italy*
³²*Nikhef National Institute for Subatomic Physics, Amsterdam, Netherlands*
³³*Nikhef National Institute for Subatomic Physics and VU University Amsterdam, Amsterdam, Netherlands*
³⁴*AGH—University of Science and Technology, Faculty of Physics and Applied Computer Science, Kraków, Poland*
³⁵*Henryk Niewodniczanski Institute of Nuclear Physics Polish Academy of Sciences, Kraków, Poland*
³⁶*National Center for Nuclear Research (NCBJ), Warsaw, Poland*
³⁷*Horia Hulubei National Institute of Physics and Nuclear Engineering, Bucharest-Magurele, Romania*
³⁸*Affiliated with an institute covered by a cooperation agreement with CERN*
³⁹*ICCUB, Universitat de Barcelona, Barcelona, Spain*
⁴⁰*Instituto Galego de Física de Altas Enerxías (IGFAE), Universidade de Santiago de Compostela, Santiago de Compostela, Spain*
⁴¹*Instituto de Física Corpuscular, Centro Mixto Universidad de Valencia—CSIC, Valencia, Spain*
⁴²*European Organization for Nuclear Research (CERN), Geneva, Switzerland*
⁴³*Institute of Physics, Ecole Polytechnique Fédérale de Lausanne (EPFL), Lausanne, Switzerland*
⁴⁴*Physik-Institut, Universität Zürich, Zürich, Switzerland*
⁴⁵*NSC Kharkiv Institute of Physics and Technology (NSC KIPT), Kharkiv, Ukraine*
⁴⁶*Institute for Nuclear Research of the National Academy of Sciences (KINR), Kyiv, Ukraine*
⁴⁷*University of Birmingham, Birmingham, United Kingdom*
⁴⁸*H.H. Wills Physics Laboratory, University of Bristol, Bristol, United Kingdom*
⁴⁹*Cavendish Laboratory, University of Cambridge, Cambridge, United Kingdom*
⁵⁰*Department of Physics, University of Warwick, Coventry, United Kingdom*
⁵¹*STFC Rutherford Appleton Laboratory, Didcot, United Kingdom*
⁵²*School of Physics and Astronomy, University of Edinburgh, Edinburgh, United Kingdom*
⁵³*School of Physics and Astronomy, University of Glasgow, Glasgow, United Kingdom*
⁵⁴*Oliver Lodge Laboratory, University of Liverpool, Liverpool, United Kingdom*
⁵⁵*Imperial College London, London, United Kingdom*
⁵⁶*Department of Physics and Astronomy, University of Manchester, Manchester, United Kingdom*
⁵⁷*Department of Physics, University of Oxford, Oxford, United Kingdom*
⁵⁸*Massachusetts Institute of Technology, Cambridge, 02139 Massachusetts, USA*
⁵⁹*University of Cincinnati, Cincinnati, 45221 Ohio, USA*
⁶⁰*University of Maryland, College Park, 20742 Maryland, USA*

- ⁶¹*Los Alamos National Laboratory (LANL), Los Alamos, 87545 New Mexico, USA*
⁶²*Syracuse University, Syracuse, New York 13244, USA*
⁶³*School of Physics and Astronomy, Monash University, Melbourne, Australia*
(associated with Department of Physics, University of Warwick, Coventry, United Kingdom)
⁶⁴*Pontifícia Universidade Católica do Rio de Janeiro (PUC-Rio), Rio de Janeiro, Brazil*
(associated with Universidade Federal do Rio de Janeiro (UFRJ), Rio de Janeiro, Brazil)
⁶⁵*Physics and Micro Electronic College, Hunan University, Changsha City, China*
(associated with Institute of Particle Physics, Central China Normal University, Wuhan, Hubei, China)
⁶⁶*Guangdong Provincial Key Laboratory of Nuclear Science, Guangdong-Hong Kong Joint Laboratory of Quantum Matter, Institute of Quantum Matter, South China Normal University, Guangzhou, China (associated with Center for High Energy Physics, Tsinghua University, Beijing, China)*
⁶⁷*Lanzhou University, Lanzhou, China*
(associated with Institute Of High Energy Physics (IHEP), Beijing, China)
⁶⁸*School of Physics and Technology, Wuhan University, Wuhan, China*
(associated with Center for High Energy Physics, Tsinghua University, Beijing, China)
⁶⁹*Departamento de Física, Universidad Nacional de Colombia, Bogota, Colombia*
(associated with LPNHE, Sorbonne Université, Paris Diderot Sorbonne Paris Cité, CNRS/IN2P3, Paris, France)
⁷⁰*Universität Bonn—Helmholtz-Institut für Strahlen und Kernphysik, Bonn, Germany (associated with Physikalisches Institut, Ruprecht-Karls-Universität Heidelberg, Heidelberg, Germany)*
⁷¹*Eotvos Lorand University, Budapest, Hungary*
(associated with European Organization for Nuclear Research (CERN), Geneva, Switzerland)
⁷²*INFN Sezione di Perugia, Perugia, Italy (associated with INFN Sezione di Ferrara, Ferrara, Italy)*
⁷³*Van Swinderen Institute, University of Groningen, Groningen, Netherlands*
(associated with Nikhef National Institute for Subatomic Physics, Amsterdam, Netherlands)
⁷⁴*Universiteit Maastricht, Maastricht, Netherlands*
(associated with Nikhef National Institute for Subatomic Physics, Amsterdam, Netherlands)
⁷⁵*Tadeusz Kosciuszko Cracow University of Technology, Cracow, Poland*
(associated with Henryk Niewodniczanski Institute of Nuclear Physics Polish Academy of Sciences, Kraków, Poland)
⁷⁶*DS4DS, La Salle, Universitat Ramon Llull, Barcelona, Spain (associated with ICCUB, Universitat de Barcelona, Barcelona, Spain)*
⁷⁷*Department of Physics and Astronomy, Uppsala University, Uppsala, Sweden*
(associated with School of Physics and Astronomy, University of Glasgow, Glasgow, United Kingdom)
⁷⁸*University of Michigan, Ann Arbor, Michigan, USA (associated with Syracuse University, Syracuse, New York 48109, USA)*

^aDeceased.

^bAlso at Università di Firenze, Firenze, Italy.

^cAlso at Scuola Normale Superiore, Pisa, Italy.

^dAlso at Università di Ferrara, Ferrara, Italy.

^eAlso at Università di Milano Bicocca, Milano, Italy.

^fAlso at Università di Bologna, Bologna, Italy.

^gAlso at Università di Genova, Genova, Italy.

^hAlso at Universidad Nacional Autónoma de Honduras, Tegucigalpa, Honduras.

ⁱAlso at Università di Bari, Bari, Italy.

^jAlso at Università di Cagliari, Cagliari, Italy.

^kAlso at Università di Perugia, Perugia, Italy.

^lAlso at Università di Roma Tor Vergata, Roma, Italy.

^mAlso at Universidade Federal do Triângulo Mineiro (UFTM), Uberaba-MG, Brazil.

ⁿAlso at Universidade de Brasília, Brasília, Brazil.

^oAlso at Hangzhou Institute for Advanced Study, UCAS, Hangzhou, China.

^pAlso at Università di Siena, Siena, Italy.

^qAlso at Università degli Studi di Milano, Milano, Italy.

^rAlso at Central South U., Changsha, China.

^sAlso at Università di Padova, Padova, Italy.

^tAlso at Excellence Cluster ORIGINS, Munich, Germany.

^uAlso at Università di Pisa, Pisa, Italy.

^vAlso at Università della Basilicata, Potenza, Italy.

^wAlso at Universidad de Alcalá, Alcalá de Henares, Spain.

^xAlso at Università di Urbino, Urbino, Italy.